Journal of Alloys and Compounds 511 (2012) 63–69

Contents lists available at ScienceDirect

Journal of Alloys and Compounds

journal homepage: www.elsevier.com/locate/jallcom

Influence of heat treatment on phase transformation of clay–iron oxide composite

Z. Orolínová [a,*], A. Mockovčiaková [a], V. Zeleňák [b], M. Myndyk [c]

[a] Institute of Geotechnics, Slovak Academy of Sciences, Watsonova 45, Košice, Slovak Republic
[b] Institute of Chemistry, Faculty of Science, P.J. Šafárik University, Moyzesova 11, Košice, Slovak Republic
[c] Faculty of Science, Technical University of Dresden, Helmholtzstraße 10, Dresden, Germany

ARTICLE INFO

Article history:
Received 28 July 2010
Received in revised form 24 June 2011
Accepted 5 August 2011
Available online 18 September 2011

Keywords:
Composite
Iron oxides
Phase transformation
X-ray diffraction
Mössbauer spectroscopy

ABSTRACT

Magnetic clay composite prepared by the method of precipitation of iron oxide onto the clay surface was subjected to a heat treatment. The presence of iron oxide phase in composite before the heating was determined by the Mössbauer spectroscopy method as γ-Fe_2O_3. Structural changes of maghemite in clay composite after heating at selected temperatures in N_2 and Ar/H_2 atmosphere were studied using Mössbauer spectroscopy, X-ray diffraction, TG/DSC and SEM methods. It was shown the full transformation of γ-Fe_2O_3 to α-Fe_2O_3 in the inert atmosphere at temperature 650 °C and only a partial transformation to Fe_3O_4 in the reductive atmosphere at 300 °C.

1. Introduction

Preparation and research of magnetic particles has a long history in the field of solid state science, and recently was focused on nanoparticles [1–3], due to their interesting optical, magnetic, electrical and catalytical properties and wide utilization, for example for preparation of magnetic fluids, biomedical applications [4], or in remediation of oil spill [5]. Most of applications require chemically stable, well-dispersed and uniformly sized particles. For this reason new technologies in synthesis and methods of analysis have been developed. One of the effective approaches for preventing particle agglomeration is to coat nanoparticles with polymers or other targeting agents, taking into account their biocompatibility. Preparation and magnetic properties of silica coated nanoparticles were studied by Mazaleyrat et al. [6], synthesis and size-modulation of silica coated maghemite nanoparticles were described by Almeida et al. [7]. Characterization of magnetite (Fe_3O_4)/polyvinyl alcohol-based nanocomposites and study of their in vitro blood compatibility were published by Bajpai et al. [8,9]. Amino acid-coated magnetic nanoparticles which might be applied to cell separation, diagnosis and targeted drug delivery for cancer therapy were investigated by Durmus et al. [10].

Surface decoration of the aluminosilicate minerals with magnetic nanoparticles had led to a new class of composite materials [11–13], which could be also used for environmental purposes as adsorbents of organic and inorganic compounds and metal ions [14,15] or as possible contrast agent in MRI of gastrointestinal tract [16].

In this work the composite material prepared by the precipitation of iron oxide on the bentonite surface was characterized. In general, it is difficult to differentiate between two synthetic magnetic iron oxides magnetite and maghemite therefore iron oxide was also prepared without the support and studied by different methods. The composite material should be used in powder catalysts or catalysts support [17] where it might be subjected to high temperatures. Because of this reason our study was focused on the possibility to change present magnetic phase by simple heat treatment. The phase transformation was studied by X-ray diffraction and Mössbauer spectroscopy methods. The thermal properties of composite were investigated by simultaneous differential scanning calorimetry (DSC) and thermogravimetric analysis (TG/DTG). The changes in physicochemical properties of the composite affected by heat treatment [18] were studied by low temperature adsorption measurements.

* Corresponding author.
E-mail address: orolinova@saske.sk (Z. Orolínová).

0925-8388/$ – see front matter © 2011 Elsevier B.V. All rights reserved.
doi:10.1016/j.jallcom.2011.08.023

2. Materials and methods

2.1. Synthesis of composite

The natural bentonite with crystalochemical formula $[Si_{7.95}Al_{0.05}][Al_{3.03}Fe_{0.22}Mg_{0.75}]O_{20}(OH)_4(Ca_{0.42}Mg_{0.04}Na_{0.01}K_{0.01})$ originated from the deposit of locality Stará Kremnička – Jelšový potok (Slovakia) [19]. The sample was isolated from the 4% water suspension of bentonite and treated by sedimentation method with the aim to obtain the monomineral fraction of montmorillonite with the particle size below 20 μm [20]. The composite material was prepared by the method of precipitation from the solution of $FeSO_4 \cdot 7H_2O$ and $FeCl_3 \cdot 6H_2O$ (with ratio of $Fe^{3+}/Fe^{2+} = 2$), according to the method described for magnetic fluids preparation [21]. First the pH of the solution was adjusted to the value 1.8 by addition of HCl and was stirred for 0.5 h and bubbled by the nitrogen in water bath at 85 °C. The bentonite was mixed into the solution of iron cations prior to the reaction with NH_4OH and its amount was adjusted in order to obtain the weight ratio 1:1. Then the dark brown suspension was stirred for half an hour. The final product was washed with deionised water, filtrated and dried at 70 °C. The pure iron oxide particles were synthesized by the same reaction.

2.2. Heating of composite

The heating of the composite in N_2 atmosphere for 2 h up to 650 °C was used to change the magnetic phase to nonmagnetic. After 2 h the sample was taken from the furnace and cooled down to room temperature. This process was realized twice.

The composite sample was also heated in Ar/H_2 atmosphere for 1.5 h up to 300 °C. After heating the sample was cooled down in furnace to the temperature 100 °C in the same atmosphere. The process of heating and cooling was realized twice. After that the sample was remained in Ar/H_2 atmosphere to reach the room temperature.

2.3. Methods of characterization

Powder X-ray diffraction (XRD) of pure iron oxide and composite patterns were recorded using a Philips PW1820 diffractometer (The Netherlands) equipped with a CuKα radiation (40 kV, 40 mA). The JCPDS PDF database was used for the phase identification.

In situ XRD measurement of the synthesized iron oxide was realized by the diffractometer Phillips X'Pert Pro (equipped with the Cu cathode with positional sensitive detector-X'Celerator) (The Netherlands) in the high temperature chamber from 25 to 980 °C in inert atmosphere (at measurement conditions 40 kV/50 mA and divergence slit 1.0°). The data were analysed using Philips Software, X'PertHigh Score with PDF-2 Database.

Mössbauer measurements were made in transmission geometry. A ^{57}Co/Rh-ray source was used. The velocity scale was calibrated relative to ^{57}Fe in Rh. Mössbauer spectral analysis software "Recoil" [22] was used for the quantitative evaluation of the spectra. The Voigt-based fitting method was applied for all spectra to determine the line positions, line widths and peak intensities.

TG/DSC curves were recorded in the synthetic flow air (20 cm^3/min) and the heating rate 9 °C/min using Netzsch STA 409PC thermal analyzer.

Morphology of the iron oxide particles and composite sample was observed by the field-emission scanning transmission electron microscope (FE-STEM) of the type JEM-2100F (JEOL Ltd., Japan). The surface morphology of the composite sample before and after the heat treatments was compared using the scanning electron microscope (SEM) of the type JSM-6400 (JEOL Ltd., Japan).

Adsorption and desorption isotherms were measured with the Micrometrics ASAP 2400 apparatus (USA) by the method of physical adsorption of nitrogen at 77 K. Experimental data were processed by the BET (Brunauer, Emmett, Teller) isotherm [23] in the range of relative pressure 0.05–0.2 p/p_0. The value of total pore volume V_a was estimated from the maximum adsorption at relative pressure close to the saturation pressure.

3. Results and discussion

The phase analysis of the synthesized iron oxide without the support, Fig. 1, showed reflections identical with two reference patterns Fe_3O_4 (JCPDS PDF 19-0629) and γ-Fe_2O_3 (JCPDS PDF 39-1346). XRD is not sensitive enough to differentiate between magnetite and maghemite phases (both of which are spinels) due to extreme similarity in crystal structure of these two phases [24]. The XRD analysis of composite materials confirmed the presence of montmorillonite as well as the Fe oxidized phase.

The Mössbauer spectroscopy is a powerful tool to distinguish between magnetic iron oxides like Fe_3O_4 (magnetite), γ-Fe_2O_3 (maghemite) and α-Fe_2O_3 (hematite) [25]. Magnetite crystallizes in the spinel structure, space group *Fd*3*m*. The oxygen ions form a

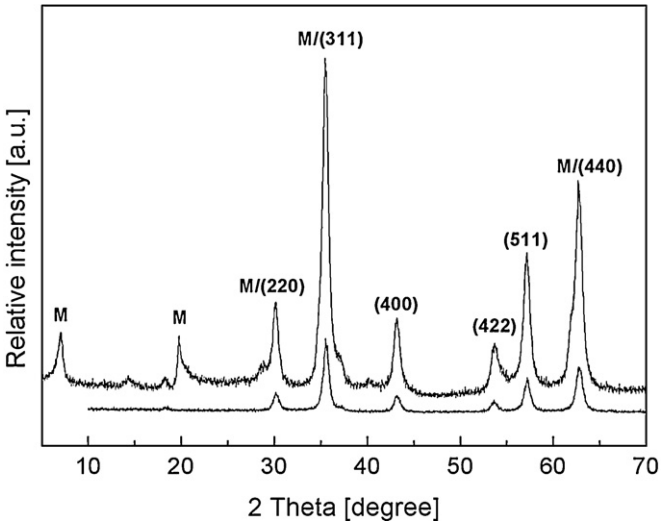

Fig. 1. XRD pattern of the synthesized iron oxide without the support and the composite material (M, montmorillonite).

closed-packed cubic lattice and the metal ions are located in the interstices between the oxygen ions. There are two kinds of interstices occupied of iron atoms: the tetrahedral (A) sites and the octahedral [B] sites. In the unit cell, there are twice as many B-sites, populated by Fe^{2+} and Fe^{3+}, as A-sites, populated by Fe^{3+}. The iron (III) oxide γ-Fe_2O_3 adopts a spinel-related structure commonly represented by the formula $(Fe)[Fe_{5/3}\Delta_{1/3}]O_4$ where ( ) denotes tetrahedral sites, [ ] indicates octahedral sites and Δ denotes vacancies [26]. The room-temperature (RT) microcrystalline maghemite is readily distinguished from bulk magnetite or nonstochiometric magnetite through the spectrum with lower hyperfine fields (and with asymmetric lines) and/or the presence of a superparamagnetic doublet [27]. In spite of the existence of ferric ions in two totally different environments, the magnetically split Mössbauer spectra of maghemite, at all temperatures, show only one broad sextet pattern, indicating, that the hyperfine parameters of both A- and B-sites are very similar in magnitude [28].

The RT Mössbauer spectrum of synthesized iron oxide sample is magnetically ordered, Fig. 2a. It consists of a sextet with broad line, not comparable with spectrum typical for magnetite. The line shape is asymmetric, so the presence of nanosized particles is expected. From this reason some assumptions on the spectrum fitting have been accepted:

1. The distribution of hyperfine magnetic field in tetrahedral position is narrow, in octahedral is broad.

   The hyperfine magnetic field of small particles depends on their size, therefore the broadening of the Mössbauer lines and/or the line shape asymmetry should be explained by the particle size distribution [29]. The spectrum, Fig. 2b, has to be fitted with a distribution of hyperfine fields.

   The asymmetric line shape and the distribution of hyperfine magnetic fields indicate the presence of magnetic particles with size bellow 100 nm (nanoparticles).
2. The parameters of the tetrahedral lines (isomer shift IS and hyperfine magnetic field *H*) are the same or less unchanged in comparison with a bulk material ($IS_{A\ nano} = IS_{A\ bulk}$, $H_{A\ nano} = H_{A\ bulk}$).
3. Based on the results [30] the cation distribution in γ-Fe_2O_3 is independent on the particle size.
4. The ratio of relative intensities of the subspectra is: $I_A:I_B = 0.6$.

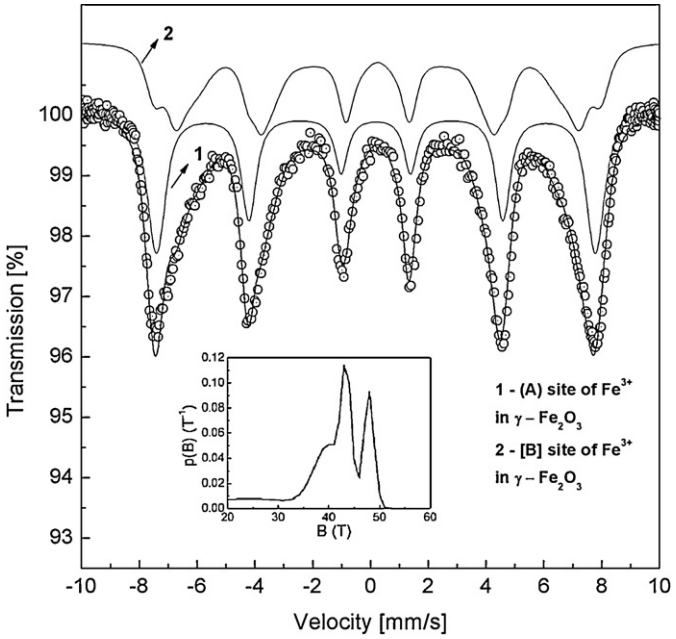

Fig. 2. Mössbauer spectrum of the synthesized iron oxide.

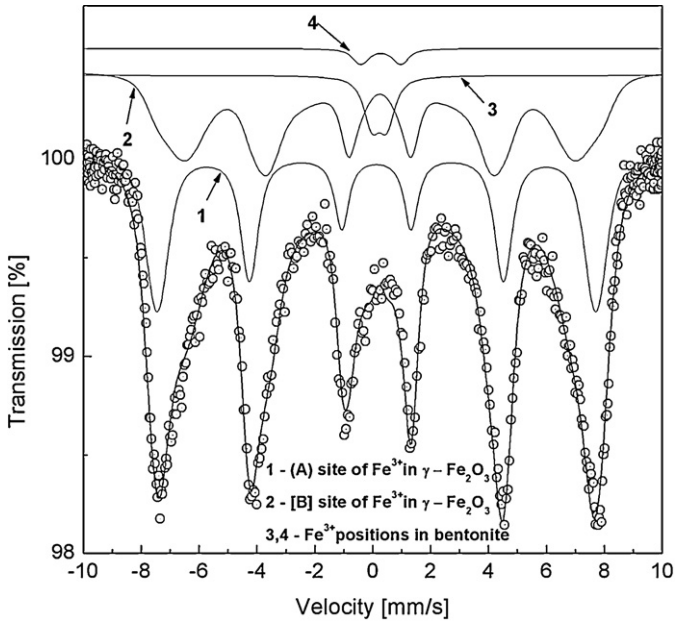

Fig. 3. Mössbauer spectrum of the composite.

The RT Mössbauer parameters obtained from the fitting, Table 1, showed only an existence of maghemite in the sample, as was published in [31]. In spite of the presence of inert atmosphere in the process of the composite synthesis (Section 2.1), the present Fe^{2+} was completely oxidized during the composite drying. Based on the results in [32] the considerable oxidation can occur due to the electron-hopping phenomena in ultrafine magnetite powders even at room temperature. The obtained values of hyperfine magnetic fields of synthesized γ-Fe_2O_3 slightly differ from the results published by Vandenberghe et al. (49.8 T for both sites) [27], Lee et al. (49.3 T for tetrahedral site, 50.2 T for octahedral) [30] or Helgason et al. (47.3 T and 53.4 T) [33]. Regarding the particles size of the synthesized iron oxide the obtained parameters are in good agreement with published values for different maghemites.

The spectrum of the composite is a complex consisting of one paramagnetic doublet and one sextet, Fig. 3. Besides the components, which belong to the synthesized iron oxide, also the presence of iron cations in the bentonite structure had to be considered. Clay minerals can contain structural iron on concentrations from less than 1% to over 10%. This is usually octahedrally, less frequently tetrahedrally, coordinated. Most clay minerals are paramagnetic down to 4.2 K [34,35]. Mössbauer spectra of clay minerals are usually broad and in dependance on the valence of iron and the number of sites in the structure, the spectra consist of one or several Fe^{2+} and/or Fe^{3+} doublets. For montmorillonite, it is often possible to fit observed spectrum with two Fe^{3+} doublets of similar chemical isomer shifts, while the more intense doublet has the quadrupole splitting approximately a half of that, which belongs to the less intense doublet [36]. For experimental data fitting superposition of four spectral components (two sextets and two doublets) was needed. The obtained parameters are listed in Table 2. Considering the presence of γ-Fe_2O_3 nanoparticles, the spectrum was also fitted with distributed hyperfine fields. The relative area of the first component of B_{hf} in octahedral site (47.9 T) is only 6.3% in comparison with 14.4% for pure oxide. It should be caused by the presence of higher amount of smaller maghemite particles in composite, what was also observed by TEM. Two positions of trivalent iron in the bentonite, which were detected probably represent central Fe^{3+} atoms in octahedrons and atoms in the interlayer space in bentonite structure.

FE-TEM micrograph of synthesized maghemite nanoparticles is shown in Fig. 4a. All the particles are approximately of the spherical shape and their size (diameters) changes in the range from 10 to 50 nm. Selected area electron diffraction pattern exhibits spots and rings indicating the presence of structurally disordered regions. Marked Debye-Sherrer rings, Fig. 4b, represent interlayer distances in the structure of the nanoparticles corresponding to the reference diffractions of γ-Fe_2O_3, what is in agreement with the result obtained from the Mössbauer spectroscopy. The nanomorphology of the composite material is shown in Fig. 5. Agglomerations of magnetic particles (sized in range from 10 to 30 nm) nonhomogenously distributed on the bentonite surface can be seen. The occurence of smaller iron oxide particles in the composite corresponds with the results obtained from the Mössbauer spectroscopy measurements discussed above.

The thermal stability of the pure nanocrystalline maghemite was studied by the in situ XRD method at various temperatures: 25, 140, 370, 430, 480, 530, 590, 775 and 980 °C, Fig. 6. Typical X-ray peaks of the maghemite spinel structure are observed

Table 1
Mössbauer parameters for synthesized iron oxide.

Spectral component	B_{hf} [T]	IS [mm/s]	RA [%]
Fe^{3+} Tetrahedral site	47.0	0.13	37.5
Fe^{3+} Octahedral site	47.9	0.25	14.4
	43.4		14.3
	40.0		21.8
	24.3		12.0

B_{hf}, hyperfine magnetic field; IS, isomer shift; RA, relative spectral area.

Table 2
Mössbauer parameters for composite material.

Spectral component	B_{hf} [T]	IS [mm/s]	QS [mm/s]	RA [%]
Fe^{3+}		0.23	0.52	3.4
Fe^{3+}		0.28	1.38	1.1
Fe^{3+} Tetrahedral site	47.0	0.13		35.8
Fe^{3+} Octahedral site	47.9	0.25		6.3
	42.0			36.2
	28.6			17.2

B_{hf}, hyperfine magnetic field; IS, isomer shift; QS, quadrupole splitting; RA, relative spectral area.

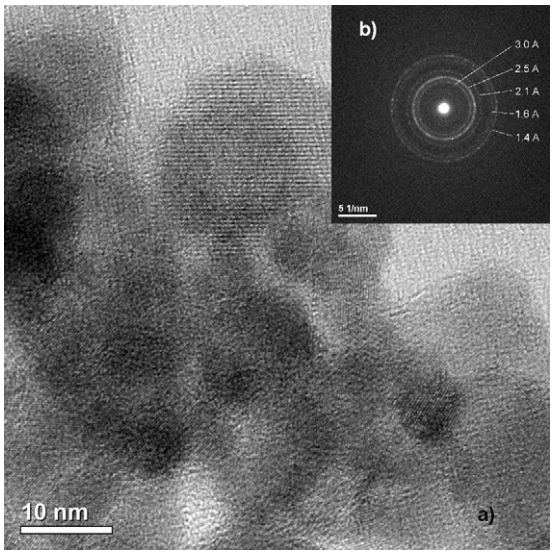

Fig. 4. FE-TEM micrograph of the synthesized maghemite (a) with electron diffraction pattern (b).

in the diffractograms of the nonheated and heated sample in the range 140–530 °C. At 590 °C the specimen is in a mix state of γ and α phases. Full phase transformation was obtained at 775 °C. Similar results were published by Sartorrato et al. [37], where diffractograms of the maghemite powder sample heated in temperature range of 700–1400 °C showed only the hematite phase. Quenched synthesized nanocrystalline γ-Fe_2O_3, studied by Ye et al. [38], was changed completely into α-Fe_2O_3 when the temperature was higher than 550 °C.

The thermogravimetric and differential scanning calorimetry curves for the composite is shown in Fig. 7. The dehydratation in the sample takes place in temperature range up to 140 °C. In temperature range from 150 to 600 °C the continuous mass loss was observed until the steeper decrease from 600 to 680 °C took place. This mass loss was accompanied with the endothermic peak on the DSC curve showing on the dehydroxylation of the composite. Upon heating, clay minerals usually become dehydroxylated and their structure break down at temperatures that are often characteristic for individual species. Önal and Sarikaya in their study observed the mass loss of the Ca-bentonite during the dehydroxylation in temperature interval from 400 to 800 °C, where the maximum temperatures for decrystallization and recrystallization were reached at 980 and 1030 °C, respectively [39]. The partial transformation

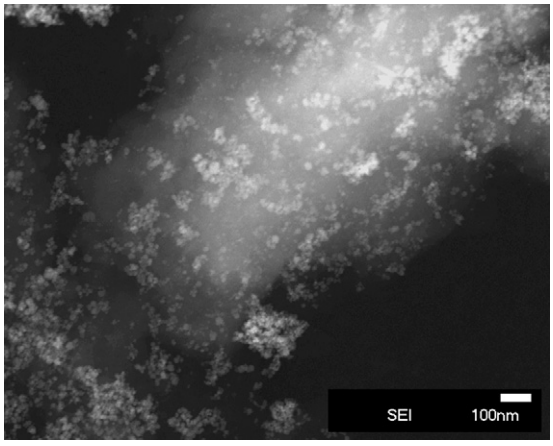

Fig. 5. FE-TEM micrograph of the composite material.

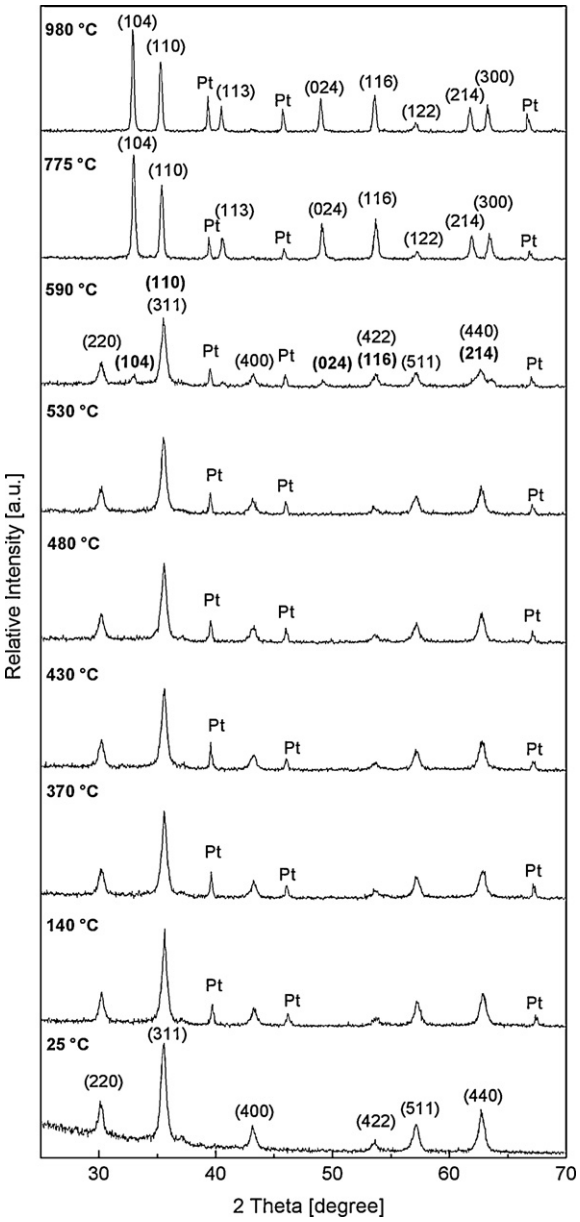

Fig. 6. In situ XRD analysis for thermal stability of the synthesized maghemite (Pt reflections belong to the platinum plate used for the measurements).

of maghemite (γ-Fe_2O_3) phase to hematite (α-Fe_2O_3) in the composite occurred at the temperature around 400 °C as indicated by a broad exothermic peak centred at 400 °C. Ennas et al. [40] also presented a broad exothermic peak centred around 390 °C in the DSC curve of the nanocrystalline γ-Fe_2O_3, corresponding to the temperature of the γ to α phase transition. Data on microcrystalline maghemite particles prepared with the conventional method showed an exothermic peak centred around 570 °C.

Based on results obtained from in situ XRD and DSC measurement, the composite was heated up to 650 °C in inert atmosphere with aim to obtain bentonite–hematite system. The XRD pattern after the thermal treatment showed narrow diffraction peaks of hematite phase (JCPDS file no.: 24-0072) pointing out well-recrystallized iron oxide particles in the composite, Fig. 8.

The RT Mössbauer spectrum of the composite heated at 650 °C showed almost symmetric sextet structure, consisting from the sharper peaks in comparison with the unheated. Three components were used for the spectrum fitting, Fig. 9: two quadrupole

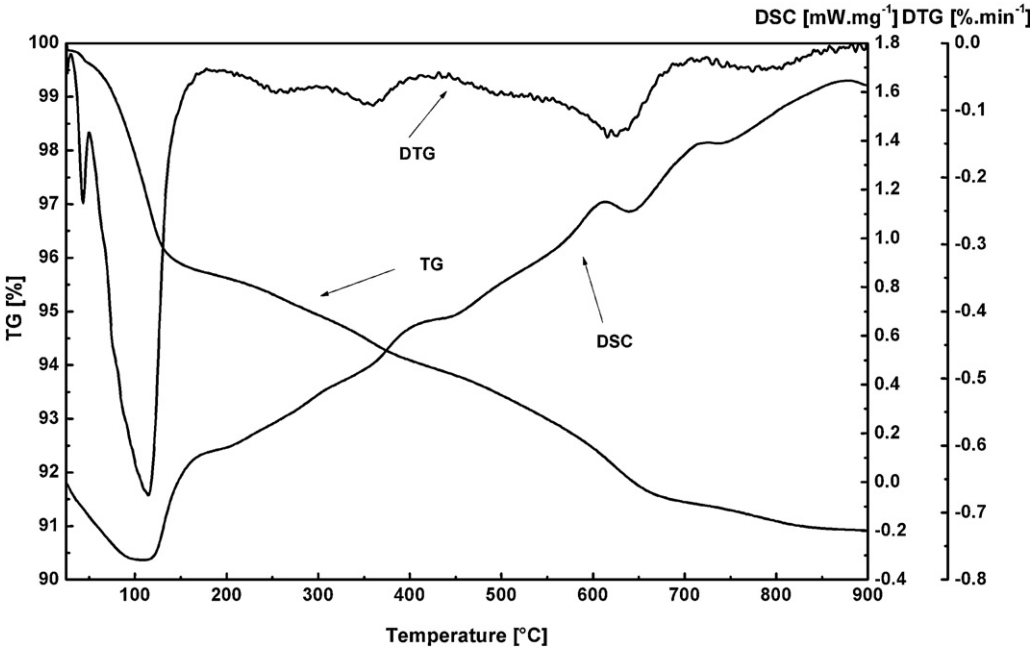

Fig. 7. TG, DTG and DSC curve of the composite sample.

spectral components for Fe^{3+} in bentonite and one sextet with distributed hyperfine fields for oxide. The obtained value of B_{hf} (50.8 T) is smaller than B_{hf} of bulk α-Fe_2O_3 (51.7 T), but is in accordance with literature date of B_{hf} for small size hematite particles (51 T) [41]. The Mössbauer parameters resulting from the fitting of the spectra, Table 3, confirmed the full transformation of γ-Fe_2O_3 to α-Fe_2O_3.

Comparison of the morphology of the composite before and after heating at 650 °C observed by SEM is shown in Fig. 10a and b. The composite after heating can be characterized by higher level of densification and homogenization.

To obtain the transformation of γ-Fe_2O_3 to Fe_3O_4 the composite was heated in reductive atmosphere at 300 °C. The XRD pattern (not shown here) recorded after this treatment did not differ significantly from the pattern of the unheated composite material, Fig. 1, due to the strong similarity in the minerals crystal structures,

Table 3
Mössbauer parameters for composite material heated at 650 °C in N_2 atmosphere.

Spectral component	B_{hf} [T]	IS [mm/s]	QS [mm/s]	RA [%]
Fe^{3+}		0.23	1.86	2.7
Fe^{3+}		0.22	0.66	2.8
Fe^{3+}	50.8	0.23	−0.1	79.1
	47.0			7.6
	39.2			7.8

B_{hf}, hyperfine magnetic field; IS, isomer shift; QS, quadrupole splitting; RA, relative spectral area.

mentioned earlier. The RT Mössbauer spectrum is asymmetric, splitting of the experimental peaks in the left part can be seen, Fig. 11. For suitable fitting five components were used, which showed, that phase transformation in this case was only partial. Contrary to the work, where nearly full transformation of maghemite to magnetite in partially oxidized basalt lava was reached [42], in our experiment approximately 1/3 of the residual

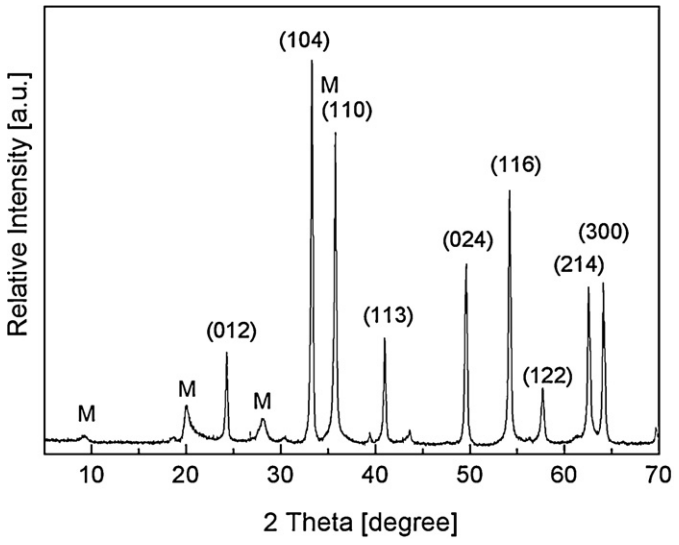

Fig. 8. XRD pattern of the composite heated up to 650 °C.

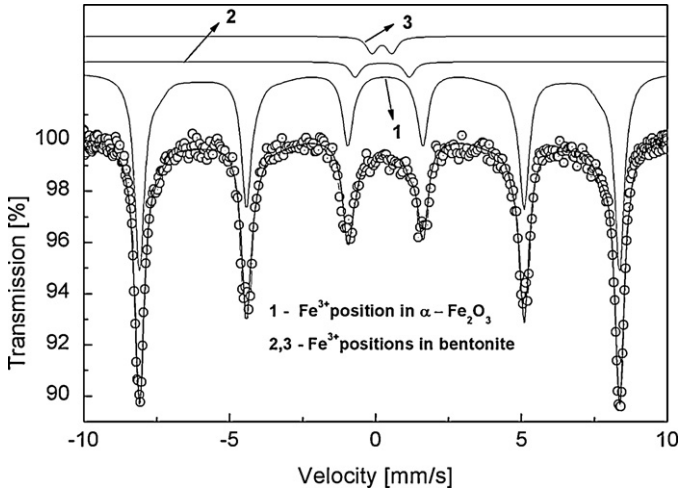

Fig. 9. Mössbauer spectrum of the composite heated up to 650 °C.

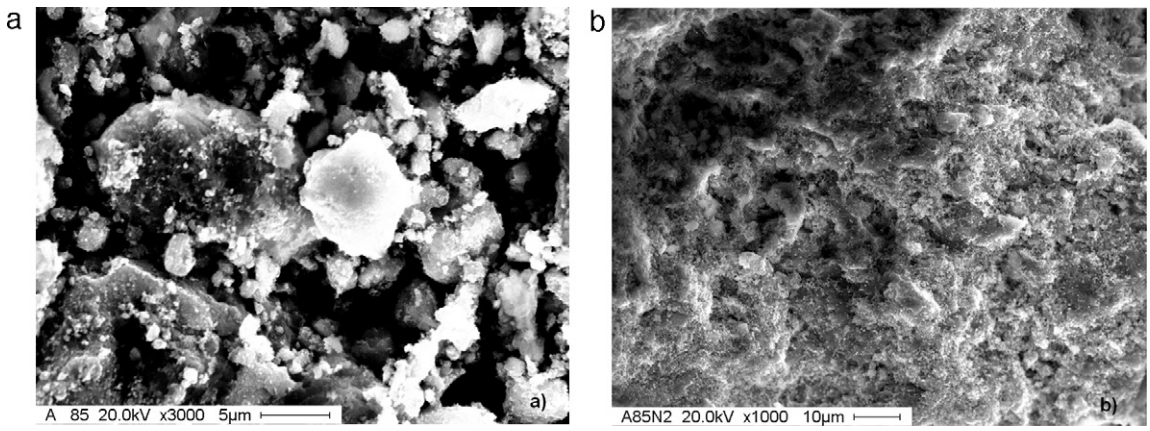

Fig. 10. SEM micrograph of the parent composite (a) and heated up to 650 °C (b).

Table 4
Mössbauer parameters for composite material heated at 300 °C in H_2/Ar atmosphere.

Spectral component	B_{hf} [T]	IS [mm/s]	QS [mm/s]	RA [%]
Fe^{3+}		0.23	0.6	1.7
Fe^{3+}		0.28	1.30	0.7
Fe^{3+} Tetrahedral site	47.1	0.13		13.1
Fe^{3+} Octahedral site	47.8	0.25		36.3
	25.9			14.6
Fe^{2+} Octahedral site	45.8	0.57		4.4
	44.1			12.8
	39.2			9.9

B_{hf}, hyperfine magnetic field; IS, isomer shift; QS, quadrupole splitting; RA, relative spectral area.

maghemite can be found in the sample. It can be probably explained by the presence of fine iron oxide particles, which are not so stable and air oxidation takes place. Obtained Mössbauer parameters are listed in Table 4.

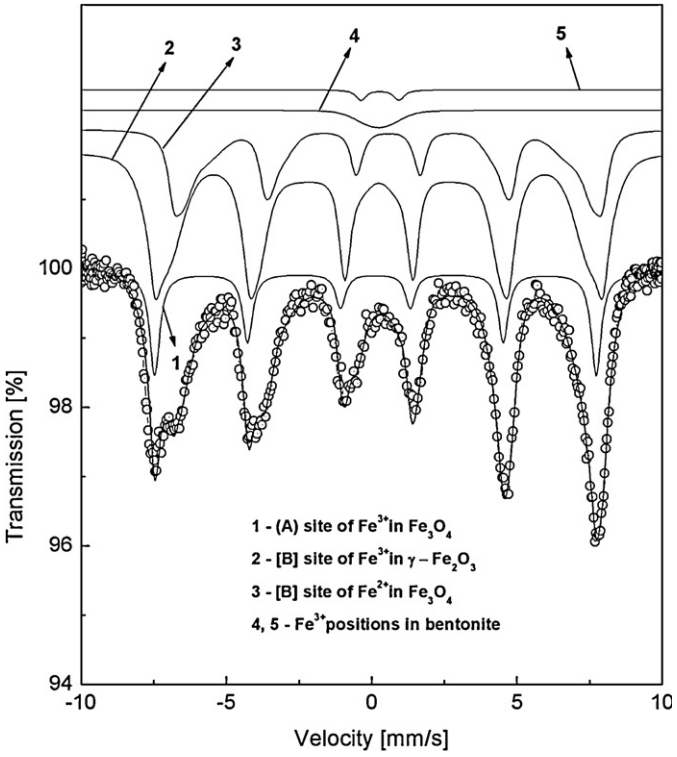

Fig. 11. Mössbauer spectrum of the composite heated up to 300 °C.

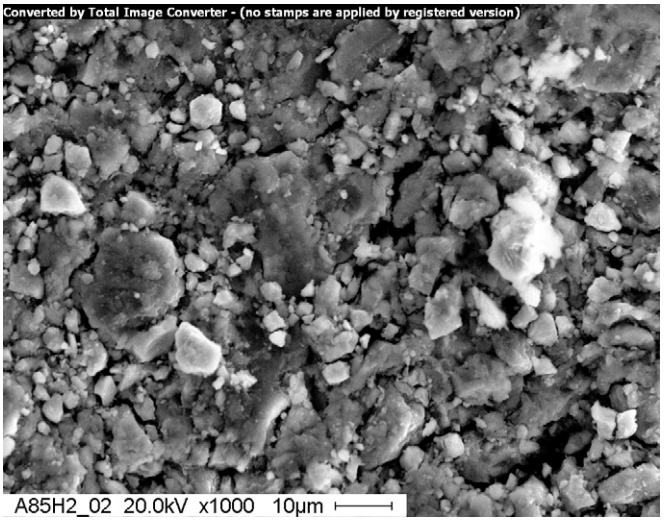

Fig. 12. SEM micrograph of the composite sample heated up to 300 °C.

Comparing the morphology of parent composite (Fig. 10a) and composite after treatment, Fig. 12, only a small difference can be observed.

Surface properties of the parent and heated composite were studied by the nitrogen adsorption method. The value of the specific surface area of the composite heated up to 650 °C decreased

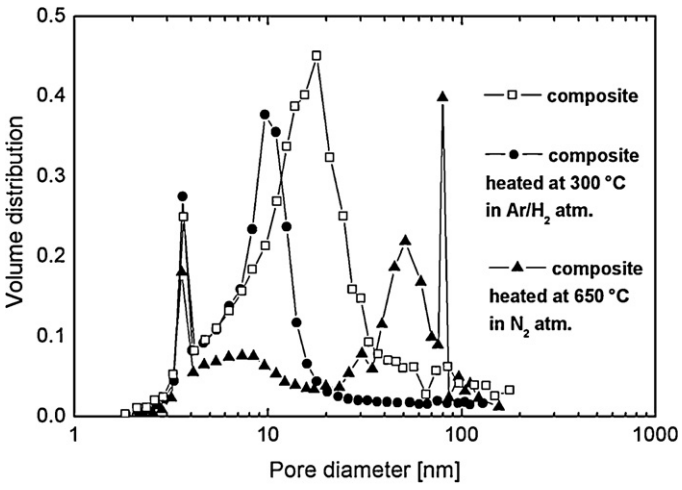

Fig. 13. Pore size distribution curves of the composite samples.

from 82.80 m^2/g to 38.46 m^2/g. This relates with the recrystallization of the iron oxide particles, observed by XRD and Mössbauer spectroscopy method. The significant change in porous structure after this treatment can be seen on the pore size distribution curves in Fig. 13. Except the mesopores, macropores are dominant in this structure. After the heating up to 300 °C only a small decrease of specific surface area was observed (75.57 m^2/g). The peak of the pore size distribution curve is narrower than the peak of the non-heated composite and is shifted left, into the range of smaller pores. The values of the total pore volume decreased from 0.251 to 0.125 cm^3/g STP and to 0.170 cm^3/g STP after the treatments at 650 and 300 °C, respectively.

4. Conclusion

It was observed that synthesized γ-Fe_2O_3 is thermal stable in inert atmosphere up to 530 °C, at 590 °C a mixture of γ and α phases was obtained. Heating of the clay composite up to 650 °C in the inert atmosphere led to the phase transformation of maghemite to α-Fe_2O_3. Due to the heating of the composite in the reductive atmosphere at 300 °C partial transformation of γ-Fe_2O_3 to Fe_3O_4 was obtained, changing slightly the magnetic properties of the composite [43]. This treatment did not influence significantly the surface parameters of the composite material, contrary to the heating up to 650 °C, which caused decrease of the surface parameters. The heating of the magnetic clay composite should cause the changes in its strength. Referring to the physico-mechanical properties of bentonite [44], the changes in strength after heating of magnetic bentonite should point out the further utilization of magnetic bentonite.

Acknowledgements

The authors are thankful for financial support of VEGA grant No. 0119/09 and APVV project No. 0728-07. Author Z.O. would like to thank to DAAD (Deutscher Akademischer Austauschdienst) for scholarship gained for a short research stay in Germany. Special thanks are addressed to Prof. Vladimír Šepelák (Karlsruhe Institute of Technology, Germany) for the interpretation of Mössbauer spectra and to Priv.-Doz. Dr. Armin Feldhoff (Leibniz University Hannover, Germany) for the FE-TEM measurements.

References

[1] S. Linderoth, S. Mørup, M.D. Bentzon, J. Mater. Sci. 30 (1995) 3142–3148.
[2] D. Vollath, D.V. Szabó, R.D. Taylor, J.O. Willis, K.E. Sickafus, Nanostruct. Mater. 6 (1995) 941–944.
[3] T. Ozkaya, M.S. Toprak, A. Baykal, H. Kavas, Y. Köseoğluc, B. Aktas, J. Alloys Compd. 472 (2009) 18–23.
[4] J. Mürbe, A. Rechtenbach, J. Töpfer, Mater. Chem. Phys. 110 (2008) 426–433.
[5] J.D. Orbel, L. Godhino, S.W. Bigger, T.M. Nguyen, L.N. Ngeh, J. Chem. Educ. 74 (1997) 1446–1448.
[6] F. Mazaleyrat, M. Ammar, M. LoBue, J.-P. Bonnet, P. Audebert, G.-Y. Wang, Y. Champion, M. Hÿtch, E. Snoeck, J. Alloys Compd. 483 (2009) 473–478.
[7] M.P.S. de Almeida, K.L. Caiado, P.P.C. Sartoratto, D.O. Cintra e Silva, A.R. Pereira, P.C. Morais, J. Alloys Compd. (2009), doi:10.1016/j.jallcom.2009.10.245.
[8] A.K. Bajpai, R. Gupta, Polym. Compos. 31 (2010) 245–255.
[9] A.K. Bajpai, R. Gupta, J. Appl. Polym. Sci. 114 (2009) 3548–3560.
[10] Z. Durmus, H. Kavas, M.S. Toprak, A. Baykal, T.K. Altınçekic, A. Aslan, A. Bozkurt, S. Coşgun, J. Alloys Compd. 484 (2009) 371–376.
[11] A.B. Bourlinos, M.A. Karakassides, A. Simopoulos, D. Petridis, Chem. Mater. 12 (2000) 2640–2645.
[12] T. Szabó, A. Bakandritsos, V. Tzitzios, S. Papp, L. Kőrösi, G. Galbács, K. Musabekov, D. Bolatova, D. Petridis, I. Dékány, Nanotechnology 18 (2007) 285602–285610.
[13] M. Mashlan, H. Bartonkova, D. Jancik, J. Tucek, P. Martinec, Hyperfine Interact. 191 (2009) 151–157.
[14] X. Peng, Z. Luan, H. Zhang, Chemosphere 63 (2006) 300–306.
[15] L.C.A. Oliveira, R.V.R.A. Rios, J.D. Fabris, K. Sapag, V.K. Garg, R.M. Lago, Appl. Clay Sci. 22 (2003) 169–177.
[16] H. Bartonkov, M. Mashlan, I. Medrik, D. Jancik, R. Zboril, Chem. Pap. 61 (2007) 413–416.
[17] T.J. Pinnavaia, Science 220 (1983) 365–371.
[18] Y. Sarikaya, M. Önal, B. Baran, T. Alemdaroğlu, Clays Clay Miner. 48 (2000) 557–562.
[19] K. Jesenák, Ľ. Kuchta, L. Guller, J. Fúsková, Miner. Slov. 29 (1997) 439–442.
[20] K. Jesenák, V. Hlavatý, Scripta Fac. Sci. Nat. Univ. Masarik. Brun. Geol. 28–29 (2000) 33–36.
[21] Š. Jakabský, M. Lovás, F. Blaško, Ussing of the ferromagnetic fluids in mineral processing, Vojenská letecká akadémia gen. Milana Rastislava Štefánika, Košice, 2004.
[22] K. Lagarec, D.G. Rancourt, Recoil-Mössbauer Spectral Analysis Software for Windows, Version 02, University of Ottawa, Department of Physics, Ottava, 1998.
[23] K.S.W. Sing, D.H. Everett, R.A.W. Haul, L. Moscou, R.A. Pierotti, J. Rouquérol, T. Siemieniewska, Pure Appl. Chem. 57 (1985) 603–619.
[24] S. Nasrazadani, H. Namduri, Spectrochim. Acta B 61 (2006) 565–571.
[25] Ö. Helgason, J.M. Greneche, F.J. Berry, F. Mosselmans, J. Phys.: Condens. Matter 15 (2003) 2907–2915.
[26] L. Häggström, H. Annersten, T. Ericsson, R. Wäppling, W. Karner, S. Bjarman, Hyperfine Interact. 5 (1978) 201–214.
[27] R.E. Vandenberghe, C.A. Baretto, G.M. da Costa, E. Van San, E. de Grave, Hyperfine Interact. 126 (2000) 247–259.
[28] G.M. da Costa, E. De Grave, R.E. Vandenberghe, Hyperfine Interact. 117 (1998) 207–243.
[29] S. Bid, A. Banerjee, S. Kumar, S.K. Pradhan, U. De, D. Banerjee, J. Alloys Compd. 326 (2001) 292–297.
[30] S.J. Lee, S. Lee, New J. Phys. 8 (2006) 98–102.
[31] Z. Orolínová, A. Mockovčiaková, Mater. Chem. Phys. 114 (2009) 956–961.
[32] K. Haneda, A.H. Morrish, J. Phys. 38 (Suppl. no. 4) (1977), C1-321–C1-323.
[33] Ö. Helgason, J.M. Greneche, F.J. Berry, S. Mørup, F. Mosselmans, J. Phys. Condens. Matter 13 (2001) 10785–10797.
[34] E. Murad, J.H. Johnston, Iron Oxides and Oxyhydroxides in Mössbauer Spectroscopy Applied to Inorganic Chemistry, vol. 2, Plenum Press, New York/London, 1987.
[35] E. Murad, Hyperfine Interact. 111 (1998) 251–259.
[36] P.J. Michael, W.R. MacWhinnie, Polyhedron 8 (1989) 2709–2718.
[37] P.P.C. Sartorrato, K.L. Caiado, R.C. Pedroza, S.W. da Silva, P.C. Morais, J. Alloys Compd. 434–435 (2007) 650–654.
[38] X. Ye, D. Lin, Z. Jiao, L. Zhang, J. Phys. D.: Appl. Phys. 31 (1998) 2739–2744.
[39] M. Önal, Y. Sarikaya, J. Therm. Anal. Calorim. 90 (2007) 167–172.
[40] G. Ennas, G. Marongiu, A. Musinu, A. Falqui, P. Ballirano, R. Caminiti, J. Mater. Res. 14 (1999) 1570–1575.
[41] A.T. Goulart, M.F. de Jesus Filho, J.D. Fabris, J.M.D. Coey, Hyperfine Interact. 83 (1994) 451–455.
[42] Ö. Helgason, H.P. Gunnlaugsson, S. Steinthorsson, Hyperfine Interact. 70 (1992) 981–984.
[43] L.C.A. Oliveira, D.I. Petkowicz, A. Smaniotto, S.B.C. Pergher, Water Res. 38 (2004) 3699–3704.
44 M. Galamboš, O. Rosskopfová, J. Kufčáková, P. Rajec, J. Radioanal, Nucl. Chem. 288 (2011) 765–777, doi:10.1007/s10967-011-0987-0.